Inorg. Chem. **2007**, *46*, 10887–10891

Crystal Structures of $Ln_4Ni_3O_8$ (Ln = La, Nd) Triple Layer T′-type Nickelates

Viktor V. Poltavets,[†] Konstantin A. Lokshin,[‡] Mark Croft,[§] Tapas K. Mandal,[†] Takeshi Egami,[‡,||] and Martha Greenblatt*,[†]

Department of Chemistry and Chemical Biology, Rutgers, The State University of New Jersey, 610 Taylor Road, Piscataway, New Jersey 08854, Department of Materials Science and Engineering, University of Tennessee, Knoxville, Tennessee 37996, Department of Physics and Astronomy, Rutgers, The State University of New Jersey, Piscataway, New Jersey 08854, Brookhaven National Synchrotron Light Source, Brookhaven National Laboratory, Upton, New York 11973, Department of Physics and Astronomy, University of Tennessee, Knoxville, Tennessee 37996, and Metals and Ceramics Division, Oak Ridge National Laboratory, Oak Ridge, Tennessee 37831

Received July 25, 2007

Single-phase $Ln_4Ni_3O_8$ (Ln = La, Nd) nickelates were synthesized and their crystal structures were determined by Rietveld refinement of powder neutron diffraction data. The crystal structures of these mixed-valent Ni^{1+}/Ni^{2+} phases belong to the T′-type and are built by intergrowth of LnO_2 fluorite layers with triple NiO_2 infinite-layer structural blocks. The major driving force of transformation of the LnO rock-salt block of the parent $Ln_4Ni_3O_{10-\delta}$ Ruddlesden–Popper phases to the fluorite arrangement in the reduced $Ln_4Ni_3O_8$ phases is attributed to internal structural stress. This transformation allows longer Ni–O bonds in $Ln_4Ni_3O_8$ without overstretching of the Ln–O bonds, especially in the equatorial plane. The observed displacement of Ni atoms from the outer NiO_2 planes toward the Ni atom of the central NiO_2 plane in $Ln_4Ni_3O_8$ is ascribed to large electrostatic repulsion from the fluorite part of the structure. X-ray absorption spectra near the K-edge of Ni suggest that the charge density on the nickel ion is similar for all members of the T′-type $Ln_{n+1}Ni_nO_{2n+2}$ homologous series, which correlates with nearly constant Ni–O bond lengths observed in all the reduced nickelates. This suggests that the formal changes in the valence state of Ni affect the covalency of the Ni–O bond.

Introduction

All known nickelates with infinite NiO_2 square-planar layers are members of the so-called T′-type $Ln_{n+1}Ni_nO_{2n+2}$ (Ln = La, Nd; $n = 2$, 3, and ∞) homologous series and are derived from the corresponding Ruddleden−Popper (RP) parent compounds, $Ln_{n+1}Ni_nO_{3n+1}$.[1,2] Besides the presence of the unique structural element, infinite NiO_2 planes, these nickelates are rare examples of the Ni^{1+}/Ni^{2+} mixed-valent state in oxides. Moreover, the electronic configuration of Ni^{1+}/Ni^{2+}, $3d^9/3d^8$, is the same as that of Cu^{2+}/Cu^{3+} in the high-temperature superconductors. The structures of the T′-type nickelates can be described as being built by stacking of alternating ($Ln/O_2/Ln$) fluorite-type layers with $Ln_{n-1}(NiO_2)_n$ infinite layer structural blocks.[1,2] Phases with the infinite layer structure ($n = \infty$) are known both for nickelates, $LnNiO_2$ (Ln = La, Nd),[3−7] and for cuprates, such as $Ca_{0.84}Sr_{0.16}CuO_2$,[8] whereas the so-called double ($n = 2$) and triple ($n = 3$) layer

* To whom correspondence should be addressed. Telephone: 732-445-3277. Fax: 732-445-5312. E-mail: martha@rutchem.rutgers.edu.
[†] Department of Chemistry and Chemical Biology, Rutgers, The State University of New Jersey.
[‡] University of Tennessee.
[§] Department of Physics and Astonomy, Rutgers, The State University of New Jersey, and Brookhaven National Laboratory.
[||] University of Tennessee, and Oak Ridge National Laboratory.

(1) Retoux, R.; Rodriguez-Carvajal, J.; Lacorre, P. *J. Solid State Chem.* **1998**, *140*, 307.
(2) Poltavets, V. V.; Lokshin, K. A.; Dikmen, S.; Croft, M.; Egami, T.; Greenblatt, M. *J. Am. Chem. Soc.* **2006**, *128*, 9050.
(3) Crespin, M.; Levitz, P.; Gatineau, L. *J. Chem. Soc., Faraday Trans.* **1983**, *79*, 1181.
(4) Levitz, P.; Crespin, M.; Gatineau, L. *J. Chem. Soc., Faraday Trans.* **1983**, *79*, 1195.
(5) Crespin, M.; Isnard, O.; Dubois, F.; Choisnet, J.; Odier, P. *J. Solid State Chem.* **2005**, *178*, 1326.
(6) Hayward, M. A.; Green, M. A.; Rosseinsky, M. J.; Sloan, J. *J. Am. Chem. Soc.* **1999**, *121*, 8843.
(7) Hayward, M. A.; Rosseinsky, M. J. *Solid State Sci.* **2003**, *5*, 839.
(8) Siegrist, T.; Zahurak, S. M.; Murphy, D. W.; Roth, R. S. *Nature (London)* **1988**, *334*, 231.

10.1021/ic701480v CCC: $37.00
Published on Web 11/07/2007

T′-type nickelates are unique examples of such structural arrangements.[1,2,9]

Recently, the preparation and the structure of the double-layer T′-type phase, $La_3Ni_2O_6$, have been reported for the first time.[2] The crystal structure of $Nd_4Ni_3O_8$ is also known, while only cell parameters are known for $La_4Ni_3O_8$.[1] The detailed structural information is crucial for understanding the properties, as well as for the design of new phases with similar structural units. In this paper we present the crystal structures of $Ln_4Ni_3O_8$ (Ln = La, Nd) determined by the Rietveld analysis of powder neutron diffraction (PND) data together with the X-ray absorption spectroscopy (XAS) data.

Experimental Section

$Ln_4Ni_3O_{10-\delta}$ (Ln = La, Nd) were synthesized by the sol−gel Pechini technique[10] as was described earlier.[11] The final sintering was performed in an oxygen flow at 1150 °C for $La_4Ni_3O_{10-\delta}$ and 950 °C for $Nd_4Ni_3O_{10-\delta}$ for 200 h with four intermittent grindings.

$La_4Ni_3O_8$ was prepared by the reduction of the $La_4Ni_3O_{10-\delta}$ powder in flowing pure hydrogen. The course of the reduction process was monitored by powder X-ray diffraction (PXD) performed in 12 h intervals. The process temperature was 350 °C at the initial stages, and subsequently it was decreased to 325 °C during the final treatments. The total reduction time was about 100 h. Similarly, reduction of the $Nd_4Ni_3O_{10-\delta}$ for 72 h at 350 °C in flowing pure H_2 resulted in the formation of $Nd_4Ni_3O_8$.

Powder neutron diffraction data were collected on 1-2 g samples at 300 K on the NPDF time-of-flight neutron diffractometer at the Lujan Neutron Science Center of the Los Alamos National Laboratory. Rietveld refinement[12] of the obtained data was performed with GSAS[13] program with EXPGUI[14] interface. In the final runs, the scale factor, unit-cell parameters, absorption coefficient, atomic coordinates, and isotropic atomic displacement parameters were simultaneously refined. The powder X-ray diffraction patterns were recorded at room temperature over an angular range of $5° \leq 2\theta \leq 90°$ with a step of 0.02° (2θ) on a Bruker D8 Advance diffractometer (Bragg−Brentano geometry, Cu Kα radiation). Thermogravimetric analysis (TGA) was performed with a TA Instrument 2050 thermal analyzer. Samples were ramped at 5 °C/min to a final temperature of 900 °C.

The Ni K-edge X-ray absorption spectroscopy measurements were performed on beam line X-19A at the Brookhaven National Synchrotron Light Source. Both fluorescence and transmission mode measurements were made. The incident and transmitted beam intensities were measured with ionization chambers and the fluorescence intensities with Canberra PIPS detectors. The relative energies between various spectra were determined with a simultaneously run standard, and, in general, the relative accuracy of the energy is about ±0.1 eV. All spectra were normalized to unity step in the absorption coefficient from well below to well above the edge.

Results and Discussion

Synthesis. The purity of the parent $Ln_4Ni_3O_{10-\delta}$ (Ln = La, Nd) RP phases was confirmed by indexing of all of the observed reflections of the PXD and PND patterns. The refined unit cell parameters of the orthorhombic $La_4Ni_3O_{10-\delta}$ phase, $a = 5.415(2)$, $b = 5.464(2)$, and $c = 27.96(1)$ Å, and for $Nd_4Ni_3O_{10-\delta}$ phase, $a = 5.359(2)$, $b = 5.452(2)$, and $c = 27.39(2)$ Å, are in good agreement with previously reported values.[15,16] The oxygen stoichiometry of these phases was determined as $La_4Ni_3O_{9.85(2)}$ and $Nd_4Ni_3O_{9.77(2)}$ by TGA in a 10% H_2/Ar flow.

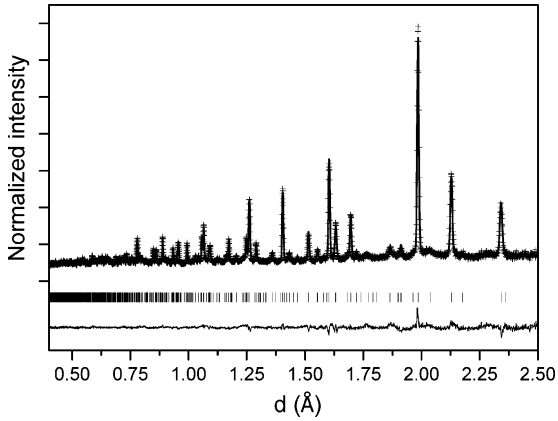

Figure 1. Rietveld refinement profiles for the PND data of $La_4Ni_3O_8$: observed intensities (crosses), calculated pattern (solid line), difference curve (bottom solid line), and Bragg positions (tick marks).

The purity of the prepared T′-type $La_4Ni_3O_8$ and $Nd_4Ni_3O_8$ phases was confirmed by indexing of all reflections on XRD and NPD patterns. The oxygen compositions, as determined by TGA, were $La_4Ni_3O_{7.98(2)}$ and $Nd_4Ni_3O_{7.99(2)}$. The oxygen content is close to the nominal one, in agreement with the line character of the phases (see below).

Crystal Structure of $La_4Ni_3O_8$ and $Nd_4Ni_3O_8$. The single-phase Rietveld refinement was carried out for the PND data of $La_4Ni_3O_8$ and $Nd_4Ni_3O_8$ in space group *I*4/*mmm* with the structural model for $Nd_4Ni_3O_8$.[1] The observed, calculated and difference profiles of the Rietveld refinement of the PND data and the refined structure of $La_4Ni_3O_8$ are shown in Figures 1 and 2, respectively. The results of the Rietveld refinement of $La_4Ni_3O_8$ and $Nd_4Ni_3O_8$ are given in Table 1 and 2, respectively.

The structures of the RP and the T′-type phases can be described as intergrowth of perovskite and rock- salt (in RP) and infinite layer and fluorite (in T′-type) structural blocks (Figure 2). The formation of the T′-type nickelates from the parent Ruddlesden−Popper phases occurs as a result of an oxygen deintercalation and a structural rearrangement in the $(LaO)_2$ part of the structure. The oxygen atoms from the LaO layers in the perovskite blocks of the parent RP phases are completely removed during the reduction process. As a consequence the distance between adjacent NiO_2 layers decreases drastically. For example, the distance between the NiO_2 planes is 3.860(2) Å in $La_4Ni_3O_{10-\delta}$ and is only 3.262-(2) Å in $La_4Ni_3O_8$. It should be noted that the $Ln_4Ni_3O_8$ structures do not allow oxygen vacancies despite their preparation by oxygen deintercalation.

(9) Lacorre, P. *J. Solid State Chem.* **1992**, *97*, 495.
(10) Pechini M. U.S. Patent 3,330,697, 1967.
(11) Poltavets, V. V.; Lokshin, K. A.; Egami, T.; Greenblatt, M. *Mater. Res. Bull.* **2006**, *41*, 955.
(12) Rietveld, H. M. *J. Appl. Crystallogr.* **1969**, *2*, 65.
(13) Larson, A. C.; Von Dreele, R. B. *Los Alamos National Laboratory Report LAUR*; Los Alamos National Laboratory: Los Alamos, NM, 2000; Vol. 86, p 748.
(14) Toby, B. H. *J. Appl. Crystallogr.* **2001**, *34*, 210.
(15) Ling, C. D.; Argyriou, D. N.; Wu, G.; Neumeier, J. J. *J. Solid State Chem.* **2000**, *152*, 517.
(16) Olafsen, A.; Fjellvag, H.; Hauback, B. C. *J. Solid State Chem.* **2000**, *151*, 46.

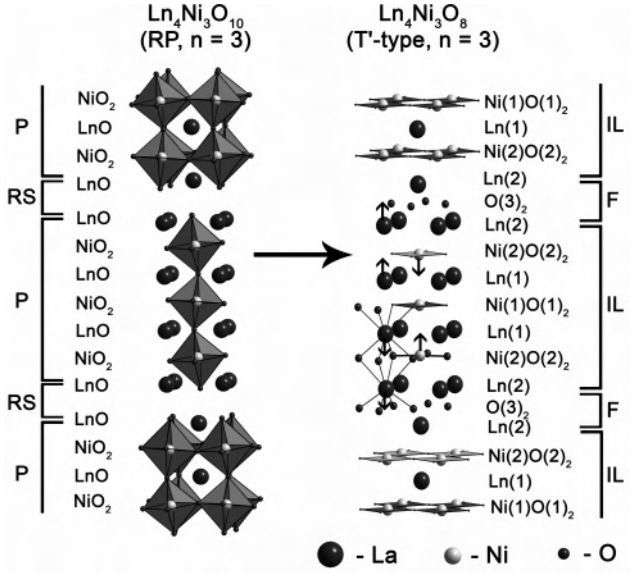

Figure 2. Structure models of $Ln_4Ni_3O_{10}$ and $Ln_4Ni_3O_8$ (Ln = La, Nd) with denoted layers and structural blocks: P, perovskite; RS, rock salt; IL, infinite layer; F, fluorite. The directions of Ln and Ni atoms shifts are shown by arrows.

Table 1. Crystallographic Data for $La_4Ni_3O_8$[a]

atom	Wyckoff position	x	y	z	10^2U_{iso} (Å^2)	occupancy
La1	4e	0	0	0.4330(1)	0.60(3)	1
La2	4e	0	0	0.2998(1)	0.78(4)	1
Ni1	2a	0	0	0	1.07(7)	1
Ni2	4e	0	0	0.1250(1)	0.72(3)	1
O1	4c	0	0.5	0	0.87(7)	1
O2	8g	0	0.5	0.1256(1)	1.18(5)	1
O3	4d	0	0.5	0.25	0.80(7)	1

[a] Space group, *I*4/*mmm* (No. 139); $a = 3.9708(1)$ Å; $c = 26.1057(5)$ Å; $\chi^2 = 2.1$; wRp = 3.7%; Rp = 2.8%.

Table 2. Crystallographic Data for $Nd_4Ni_3O_8$[a]

atom	Wyckoff position	x	y	z	10^2U_{iso} (Å^2)	occupancy
Nd1	4e	0	0	0.4343(1)	0.47(2)	1
Nd2	4e	0	0	0.2982(1)	0.56(2)	1
Ni1	2a	0	0	0	0.70(4)	1
Ni2	4e	0	0	0.1244(1)	0.74(3)	1
O1	4c	0	0.5	0	0.91(5)	1
O2	8g	0	0.5	0.1262(1)	1.08(4)	1
O3	4d	0	0.5	0.25	0.79(5)	1

[a] Space group, *I*4/*mmm* (No. 139); $a = 3.9146(1)$ Å; $c = 25.2947(5)$Å; $\chi^2 = 2.8$; wRp = 3.8%; Rp = 2.7%.

A distinctive feature of the $Ln_4Ni_3O_8$ structure is that the first coordination spheres of all Ln atoms consist of eight oxygen anions. While the average Ln−O distances are similar for both crystallographic positions (Table 3), Ln atoms are positioned asymmetrically inside their oxygen polyhedrons. The second coordination sphere of Ln depends on whether the Ln ion belongs to the infinite layer or to the fluorite part of the structure. In the fluorite block Ln(2) layers are shifted relative to each other by half of the unit cell in the [110] direction. Therefore Ln(2) ions are not exposed directly to electrostatic repulsion from other Ln(2) layers.

Table 3. Selected Interatomic Distances and Bond Valence Sums[a]

substance	in infinite layer blocks		in fluorite blocks	
$La_4Ni_3O_8$				
Ln−O dist (Å)	La(1)−O(1)	4 × 2.647(2)	La(2)−O(2)	4 × 2.782(3)
	La(1)−O(2)	4 × 2.505(3)	La(2)−O(3)	4 × 2.373(1)
av Ln−O dist (Å)	La(1)−O	2.576(3)	La(2)−O	2.5775(3)
BVS	La(1)	2.73	La(2)	3.09
$Nd_4Ni_3O_8$				
Ln−O dist (Å)	Nd(1)−O(1)	4 × 2.568(2)	Nd(2)−O(2)	4 × 2.737(2)
	Nd(1)−O(2)	4 × 2.484(2)	Nd(2)−O(3)	4 × 2.306(1)
av Ln−O dist (Å)	Nd(1)−O	2.526(2)	Nd(2)−O	2.5215(2)
BVS	Nd(1)	2.67	Nd(2)	3.15

[a] BVS = bond valence sum.

The Ln(2) ions are associated with one Ln(1) and four Ni(2) cations in the second coordination sphere from the adjacent infinite layer part of the structure. Thus Ln(2) is exposed to asymmetric electrostatic repulsions, which results in the Ln(2)−O(3) distance being shorter than the Ln(2)−O(2) distance by more than 0.4 Å. The asymmetry of Ln(2) in the first oxygen coordination sphere leads, to a smaller degree, in the asymmetric position of Ln(1) ions in the infinite layer block. The Ln(1)−O(1) bond is longer than Ln(1)−O(2) by about 0.15 Å. The directions of the displacements of the ions relative to their symmetric position in the first coordination polyhedral are depicted in Figure 2.

The average Ln−O distances in $Ln_4Ni_3O_8$ are similar for both of the rare earth cation positions, but the bond valence sum (BVS) values[17] differ substantially (Table 3). The BVS value for Ln is expected to be close to its formal oxidation state 3+, which is valid for Ln(2). However, BVS values calculated for Ln(1) are significantly lower, 2.67 and 2.73 for $Nd_4Ni_3O_8$ and for $La_4Ni_3O_8$, respectively. Relatively low BVS values for Ln in the infinite layer part of the structure seem to be typical for the whole $Ln_{n+1}Ni_nO_{2n+2}$ series. Namely, BVS for La is equal to 2.80 in $La_3Ni_2O_6$[2] and 2.51 in $LaNiO_2$.[6] Such a significant deviation of BVS values from 3 seems to be related to a remarkable feature in this homologues series. Namely, the *a* unit-cell parameters, and consequently the Ni−O bond lengths, are similar for all homologues. This is especially surprising considering the large range of formal Ni oxidation states in these compounds. For example, the *a* parameters for $LaNi^{1+}O_2$, $La_4Ni^{1.33+}{}_3O_8$ and $La_3Ni^{1.5+}{}_2O_6$ are 3.959(1),[5,6] 3.9708(1) [this Article], and 3.9686(1) Å.[2] Such deviation of BVS from 3+ can be attributed to internal strain within the structure[18] or to changes in the Ni−O bonding character. Indeed, the XAS spectra suggest increased covalency in the Ni−O bond upon reduction.

Another interesting feature found in $Ln_4Ni_3O_8$ structures is the displacement of the Ni(2) atoms out of the NiO_2 planes, as shown in Figure 2. Note that the Ni(2) atoms are shifted toward the Ni(1) atoms, which is opposite to the direction that one would expect taking into consideration electrostatic interactions of Ni(2) with its first three coordination spheres. The absolute value of the Ni(2) displacement relative to the O(2) layer is equal to 0.015 Å in $La_4Ni_3O_8$ and 0.045 Å in $Nd_4Ni_3O_8$, resulting in the O(2)−Ni(2)−O(2) angle of 179.1-

(17) Brese, N. E.; O'keeffe, M. *Acta Crystallogr., Sect. B* **1991**, *47*, 192.
(18) Brown, I. D. *J. Solid State Chem.* **1991**, *90*, 155.

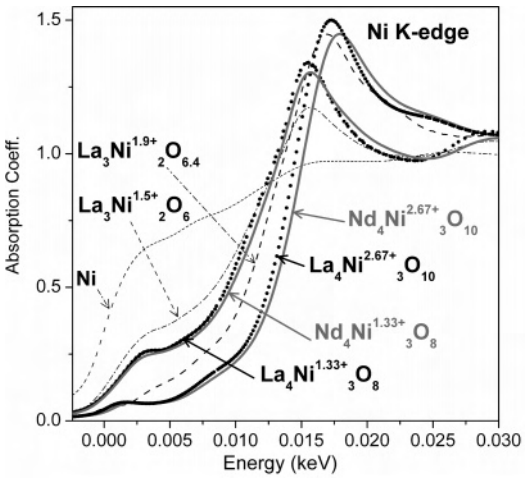

Figure 3. X-ray absorption spectra for $Ln_4Ni_3O_8$ (Ln = La, Nd) and for standards.

(1) and 177.3(1)°, respectively. The most probable explanation of the direction of the Ni(2) displacement is that the electrostatic repulsion of positively charged $Ni^{1.33+}$(2) with the fluorite block is stronger then that with the infinite layer block. However, we cannot completely rule out the possibility of direct Ni(1)−Ni(2) interaction because the distance between the Jahn−Teller cations (Ni^{1+}) is relatively short, 3.15 and 3.26 Å, for $Nd_4Ni_3O_8$ and $La_4Ni_3O_8$, respectively.

XAS Results on Ni Reduction. To confirm the evolution of the Ni oxidation states in these nickelates, Ni K-edge X-ray absorption spectroscopy measurements (see Figure 3) were performed. The standard compounds, elemental-Ni^0, $La_3Ni^{1.5+}{}_2O_6$, and $La_3Ni^{1.9+}{}_2O_{6.4}$[2] illustrate the changing structure and chemical shift accompanying Ni valence variation. The chemical shift to lower energy with increasing Ni reduction can be seen by the displacement of the standard curves at the normalized absorption coefficient (μ) value of about 0.5. In the case of Ni-reduction with significant Ni^{1+} admixture, a distinctive down-shifted shoulder feature develops in the 0−5 eV range. This shoulder feature is similar to that which develops with increasing Cu^{1+} admixture in cuprates.[19,20] In the cuprates with structures where there has been apical O removal, such a strong low-energy feature is associated with $4p_\pi$ states along the missing O-direction with d^{10} and d^{10} L character (where the L denotes an O-ligand hole). By analogy, this Ni−K feature is associated with $4p_\pi$ d^9 and d^9 L states directed along the missing O sites in this O-deficient compound. Finally it should be pointed out that the intensity at the highest spectral peak (in the 0.013−0.020 keV) decreases upon Ni valence reduction.

It is worth noting that the main peak (in the 0.013−0.020 keV) systematicly broadens (on the high-energy side), decreases in height, and shifts to slightly higher energy in the Nd compounds relative to the La compounds. This is true for both RP parent and square-planar reduced T′-type compounds. Presumably these modifications are related to larger distribution of Ni coordination environments in the more distorted Nd compounds in comparison with the La ones.

The parent RP $Ln_4Ni_3O_{10}$ spectra in Figure 3 are shifted quite significantly up in energy relative to the $Ni^{1.9+}$ standard consistent with their formal $Ni^{2.67+}$ valence state. The reduced T′-type compound $Ln_4Ni_3O_8$ spectra are dramatically down-shifted in energy and developed a distinctive shoulder feature (noted above). It is worth noting that the peak intensity also manifests the characteristic decrease in the reduced phase relative to the RP parent compounds. Thus the Ni−K XAS results clearly indicate Ni^{1+} admixture consistent with expectation from the missing O coordination as required by the structure determination.

Driving Force of T−T′ Transition. It was suggested that the preference of Ni cations for the square-planar environment and the smaller Ln cations for 8-fold coordination are important factors for the T-to-T′-structure rearrangement in nickelates.[1,21] Moreover, in adjacent layers the bond lengths should match to provide structural stability. Mismatch in bond lengths may be tolerated to some extent by bonds stretching/compressing and/or some other type of structural deformation. Such internal stress may be decreased in the perovskite part of the RP structure by octahedral tilting, but there is no stress release mechanism for the rock-salt part of the structure.

For the rare earth elements in the rock-salt layer of $Ln_4Ni_3O_{10-\delta}$ the average Ln−O bond lengths are in good agreement with the expected ones.[22] For example, the average observed La−O distance is 2.63 Å [15] in comparison with the expected 2.62 Å.[22] These values for Nd−O distances are 2.60 Å [16] and 2.56 Å.[22] In contrast, the average Ln−O bond lengths to the four oxygen atoms of the same LnO plane in the RS block are much longer, 2.75 Å for both the La and Nd compounds. The longest in-plane Ln−O bonds are about 3 Å, making the Ln atoms 8-fold coordinated. Even if we ignore the longest Ln−O bonds, the second longest ones still lie in the LnO planes. It is evident that the Ln−O bonds are substantially stretched in the LnO planes of the RP phases. As a result of the reduction of $Ln_4Ni_3O_{10-\delta}$ to $Ln_4Ni_3O_8$ the formal average oxidation state of Ni decreases from 2.67 to 1.33; consequently the ionic radii of Ni cations strongly increase, and the degree of in plane Ln−O bond stretching would be expected to become even larger in the reduced phases.

However, this internal structural stress is partially released by the transformation from rock salt to the fluorite arrangement (so-called T-to-T′-type transition). In spite of the larger in plane Ni−O distances in the reduced phases, the average Ln−O bond lengths are smaller (Table 3). In addition, there are no unusually long Ln−O bonds as in the parent (RP) structure. Therefore we suggest that the internal structural

(19) Tranquada, J. M.; Heald, S. M.; Moodenbaugh, A. R.; Liang, G.; Croft, M. *Nature* **1989**, *337*, 720.
(20) Liang, G.; Guo, Y.; Badresingh, D.; Xu, W.; Tang, Y.; Croft, M.; Chen, J.; Sahiner, A.; Beom-hoan, O.; Markert, J. T. *Phys. Rev. B* **1995**, *51*, 1258.
(21) Manthiram, A.; Tang, J. P.; Manivannan, V. *J. Solid State Chem.* **1999**, *148*, 499.
(22) Shannon, R. D. *Acta Crystallogr., Sect. A* **1976**, *32*, 751.

stress is the major driving force of transformation of the rock-salt block of the parent RP phases to the fluorite arrangement in the reduced phases. This transformation is a mechanism for the release of structural stress, and it allows the formation of longer Ni−O bonds required in the reduced phase. Needless to say that the preference of Ni cations for square-planar coordination is also an important factor for T′-type structure stability.

Acknowledgment. This work was supported by the National Science Foundation through Grants DMR-0233697 and DMR-0541911 at Rutgers and Grant DMR-0404781 at the University of Tennessee.

Supporting Information Available: Crystallographic information file for $Ln_4Ni_3O_8$ (Ln = La, Nd). This material is available free of charge via the Internet at http://pubs.acs.org.

IC701480V